JOURNAL OF ENVIRONMENTAL SCIENCES 124 (2023) 923–932

Available online at www.sciencedirect.com

ScienceDirect

www.elsevier.com/locate/jes

JES JOURNAL OF ENVIRONMENTAL SCIENCES

www.jesc.ac.cn

Assessing outdoor air quality vertically in an urban street canyon and its response to microclimatic factors

Chunping Miao[1,2], *Shuai Yu*[1,2], *Yue Zhang*[1,2], *Yuanman Hu*[1], *Xingyuan He*[1,2,*], *Wei Chen*[1,2,*]

[1] *CAS Key Laboratory of Forest Ecology and Management, Institute of Applied Ecology, Chinese Academy of Sciences, Shenyang 110016, China*

[2] *Shenyang Arboretum, Chinese Academy of Sciences, Shenyang 110016, China*

ARTICLE INFO

Article history:
Received 28 October 2021
Revised 9 January 2022
Accepted 12 February 2022
Available online 26 February 2022

Keywords:
Urban air pollution
Built environment
Urban form
Urbanization

ABSTRACT

The vertical distribution of air pollutants in urban street canyons is closely related to residents' health. However, the vertical air quality in urban street canyons has rarely been assessed using field observations obtained throughout the year. Therefore, this study investigated the seasonal and annual concentrations of particulate matter ($PM_{2.5}$ and PM_{10}), CO, NO_2, SO_2, O_3, air quality index, and their responses to microclimatic factors at three height levels (1.5, 27, and 69 m above street level) in an urban street canyon. The PM concentration was higher at 27 m than at 1.5 m in winter, whereas the situation was reversed in other seasons. It was found that photochemical pollutants such as NO_2 and O_3 were the primary pollutants in the urban street canyon. The days on which O_3 was the primary pollutant at the height of 1.5 m accounted for 81.07% of the entire year. The days on which NO_2 was the primary pollutant at the height of 27 and 69 m accounted for 82.49% and 72.33% of the entire year, respectively. Substantially higher concentrations of NO_2 and O_3 were found at the height of 27 m than at 69 m. In-canyon concentrations of NO_2 and O_3 were strongly correlated with air temperature, wind speed, and wind direction, which played important roles in photochemical reactions and pollutant dispersion.

Introduction

Rapid urbanization and industrialization have resulted in traffic congestion and deterioration of air quality in built environments (Tao et al., 2020; Wu et al., 2021). Air pollution in high-density urban areas has become a major threat to public health (Yang et al., 2020). Urban street canyons are one of the most important characteristics and spatial forms of cities, and street (canyon morphology affects in-canyon wind flow that ultimately influences air pollutant dispersion (Miao et al., 2020a; Miao et al., 2020b; Oke, 1988; Voordeckers et al., 2021a). For example, on the leeward side of a street canyon, the concentration of air pollutants increases with increase of the angle between wind direction and the street axis, whereas the concentration on the windward side is lowest when the street is parallel to the wind direction (Huang et al., 2019).

* Corresponding authors.
E-mails: hexy@iae.ac.cn (X. He), chenwei@iae.ac.cn (W. Chen).

https://doi.org/10.1016/j.jes.2022.02.021
1001-0742/

Poor spatial configuration and the internal composition of street canyons could reduce the self-purification effect of urban ventilation, thereby increasing local air pollutant concentrations in indoor and outdoor spaces (Miao et al., 2020a). Therefore, it is necessary to understand air pollutant dispersion within street canyons in consideration of outdoor air quality improvement and public health protection (Fu et al., 2020; Hassan et al., 2020).

The distribution of air pollutants in street canyons results from complex interactions between numerous factors that include street canyon morphology (e.g. aspect ratio (AR), sky view factor, building volume, and roof shape), green spaces (e.g. street trees, vegetation barriers, green walls, and green roofs), microclimatic factors, traffic emissions, background pollutant concentrations, pollution sources, physical processes and photochemical reactions (Abhijith et al., 2017; Moradpour et al., 2018; Wen and Malki-Epshtein, 2018; He and Gao, 2021; Tomson et al., 2021). Many recent studies have analyzed the horizontal distribution of air pollutants and the associated impact factors in street canyons (Ming et al., 2021) Miao et al. (2020a). investigated the influence of street canyon morphology and microclimatic factors on near-ground air pollutants across cities and found positive correlation between particulate matter (PM) and both sky view factor and relative humidity, whereas negative correlations were found between PM and AR, air temperature, and wind direction (Miao et al., 2020a). Voordeckers et al. (2021b) conducted city-wide analysis and found significant correlation between NO_2 and maximum hourly traffic volume. Miao et al. (2021) reported that coarse PM decreased and fine PM increased in street canyons with street trees. In addition to fixed-site measurements, mobile monitoring has been used to investigate near-ground air pollutant dispersion in urban areas (Li et al., 2018; Shi et al., 2018; Deshmukh et al., 2020).

The vertical distribution of air pollutants was found closely related to the health of residents along both sides of street canyons, and such research has been conducive to understanding the mixing processes that occur in association with the physicochemical conversion of air pollutants in street canyons (Minarro et al., 2012; Eeftens et al., 2019). Although numerous approaches have been applied to observation of vertical distribution of air pollutants, such studies have generally involved limited observation time (e.g., kites, tethered balloons and unmanned aerial vehicles), limited accuracy (e.g., LiDAR and nadir), or were unsuitable for street canyon environments (e.g., towers). For example, on the basis of two 14-days observation periods, Eeftens et al. (2019) analyzed NO_2 concentration at three different floors levels and found the highest NO_2 concentration at ground level. Lu et al. (2020) and Zheng et al. (2021) conducted field investigations to assess the vertical profile of traffic-related pollutants in built environments. However, the observation time was limited to only several days or morning in winter and afternoons in summer. Short-term observations cannot fully represent the air pollutant distribution in street canyons; thus, their research focused on the distribution of PM and CO, while photochemical pollutants such as NO_x and O_3 were rarely considered.

Although some recent studies have assessed the vertical distribution of air pollutants in urban street canyons, three primary problems remain: 1) lack of long-term observational data, 2) lack of comprehensive evaluation of various air pollutants including PM and photochemical pollutants, and 3) lack of knowledge regarding the relationship between the vertical distribution of air pollutants and microclimatic factors. These knowledge gaps limit the overall understanding of major pollutant assessment and air pollutant dispersion, obstruct the cognition of indoor/outdoor air quality, and hinder formulation of planning guidelines regarding public health in built environments.

To address the above problems, we installed observation instruments at different height levels (1.5, 27, and 69 m) in an urban street canyon of a residential area to record concentrations of $PM_{2.5}$, PM_{10}, CO, NO_2, SO_2, and O_3 and microclimatic factors (i.e., wind speed, wind direction, air temperature, relative humidity, and atmospheric pressure). The acquired data were used to analyze the seasonal and annual distributions of air pollutants and to investigate their response to microclimatic factors. The results derived from this unprecedented dataset provide new understanding regarding the drivers of outdoor air quality, and could support urban planners in developing guidelines regarding air quality improvement in built environments.

1. Materials and methods

1.1. Study site

This study was conducted in Shenyang (41°11′51″–43°02′13″N, 122°25′09″–123°48′24″E; Fig. 1A), which is a city located in northeastern China. It covers an area of 12,948 km^2 and the urbanized area is 3495 km^2 (Wu et al., 2021). The region is characterized by a mid-temperate continental climate, with annual average temperature of 8.4°C and annual average rainfall of approximately 510–680 mm. Shenyang experiences air pollution because it is a major heavy industry base in China (Wu et al., 2021). During the first half of 2020, 30.8% of days were classified as polluted. Among these polluted days, the days when either $PM_{2.5}$, O_3, or PM_{10} was the primary pollutant accounted for 67.9%, 25.0%, and 7.1%, respectively (Liaoning Shenyang Ecological Environment Monitoring Center, 2020).

1.2. Measurements

A fixed observation site was placed on Wuai Street (Fig. 1C), which is located in the main residential area of the city. The street (width: 35 m, length: 776 m) has N–S orientation with four lanes of traffic in each direction. The street is delimited by traffic lights at both ends. The average building height to the west and to the east of the street is 43.88 and 20.83 m, respectively. The buildings along both sides of the street are connected to each other by walls or stores. Observation sites were located at the center of a building (length: 89 m) to ensure their representativeness, and they were located along the façade of a building (height: 69 m) to the east of the street, which was 225 m from the north end of the street and 551 m from the south end of the street. The height of the building opposite the observation site was 92.4 m.

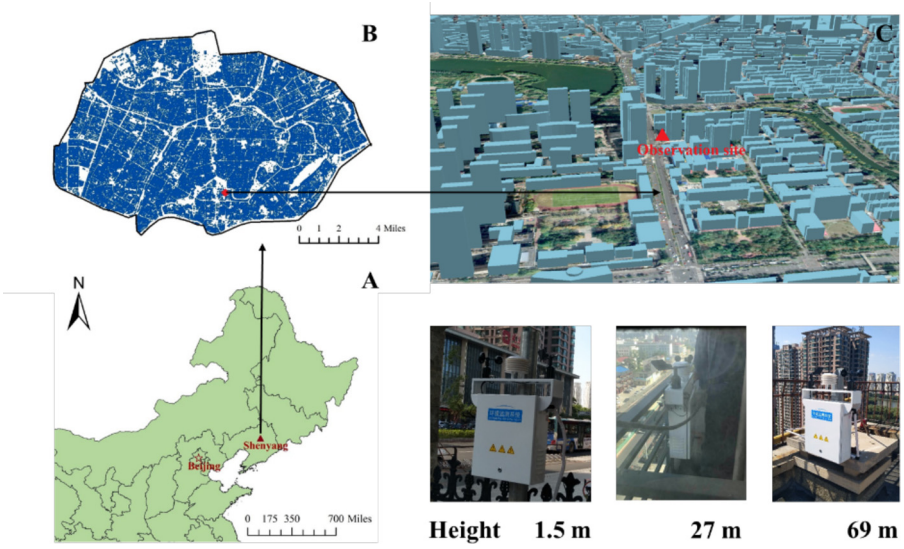

Fig. 1 – Location of the observational site on Wuai Street in Shenyang, China.

The $PM_{2.5}$, PM_{10}, CO, NO_2, SO_2, and O_3 concentrations and the microclimatic factors (instantaneous wind speed, wind direction, air temperature, relative humidity, and atmospheric pressure) were collected from December 2018 to November 2019 at three height levels: pedestrian level (1.5 m above ground level), middle level (27 m above ground level), and roof level (69 m above ground level). The air pollutant concentrations at 1.5 m represent the pedestrian pollutant exposure concentration in the street canyon. The air pollutant concentrations at 27m represent air pollution distribution at the middle level within the street canyon. The concentrations at roof level were observed to compare the differences between the air inside and outside of the canyon to elucidate air pollutant exchange and dispersion. Measurements were performed using a U-Sky outdoor environmental monitoring terminal (Shanghai lanju, China). The accuracy was ±10 μg/m^3 for both $PM_{2.5}$ and PM_{10}, ±40 ppb for NO_2, SO_2 and CO, ±0.3 ppm for O_3, ±0.3 m/sec for wind speed, ±2° for wind direction, ±0.5°C for air temperature, ±0.5% for relative humidity, and ±5% fps for atmospheric pressure. The accuracy of this monitoring terminal is suitable for the scientific research after comparing with other monitors such as Aerocet 831 (METOne Instruments, Inc., USA) and Aeroqual Series 500 portable gas monitor (Auckland, New Zealand) (Miao et al., 2020a).

1.3. *AQI index*

The air quality index (AQI) is used in many countries to assess air quality and to provide information to support the development of pollution mitigation guidelines (Tan et al., 2021). It is calculated by changing the weight significance to a particular range or set of numbers for various pollutants (Ding et al., 2021). In this study, the AQI was calculated by simplifying the concentration of six air pollutants ($PM_{2.5}$, PM_{10}, SO_2, NO_2, O_3, and CO) according to the ambient air quality standards of China (HJ633-2012). The AQI has been categorized into different classes: I (AQI: 0–50), II (AQI: 51–100), III (AQI: 101–150), IV (AQI: 151–200), V (AQI: 201–300) and VI (AQI: 301–greater), which indicates air quality are excellent, good, lightly polluted, moderately polluted, heavy polluted, and severely polluted air quality, respectively Eqs. (1) and (2)

$$IAQI_p = \frac{IAQI_{Hi} - IAQI_{Lo}}{BP_{Hi} - BP_{Lo}}(C_p - BP_{Lo}) + IAQI_{Lo} \quad (1)$$

$$AQI = \max\{IAQI_1, IAQI_2, \cdots, IAQI_n\} \quad (2)$$

where $IAQI_p$ is the air quality index of air pollutant p, C_p is the concentration of air pollutant p, BP_{Hi} represents the AQI values at the upper limits of an AQI category, BP_{Lo} represents the AQI values at the lower limits of an AQI category, $IAQI_{Hi}$ is the breakpoint concentrations of pollutant p at the upper limits of an AQI category, and $IAQI_{Lo}$ is the breakpoint concentration of pollutant p at the lower limits of an AQI category. The air quality index of the air pollutants and the corresponding pollutant concentration limits can be found in Appendix A.

1.4. *Data analysis*

The differences in $PM_{2.5}$, PM_{10}, SO_2, NO_2, CO, and the AQI in spring (March–May), summer (June–August), autumn (September–November), winter (December–February) and annually were compared. Pairwise Pearson's correlation coefficients were calculated between pairs of data of $PM_{2.5}$, PM_{10}, SO_2, NO_2, CO, AQI, atmospheric pressure, air temperature, relative humidity, wind speed, and wind direction at the three height levels on clean days (AQI≤100) and on polluted days (AQI>100) according to the AQI values calculated based on the data collected in this study. The Pearson's correlation test were performed following implementation of a normality test and significance was assessed at the level of $p < 0.05$ (Eslami and Saeed, 2018).

We also performed canonical correspondence analysis (CCA) to further assess the influence of microclimatic factors on air quality at the three height levels. CCA is an ordination method suitable for multivariate direct gradient analysis (Terbraak, 1986). It is a unimodal response model that as-

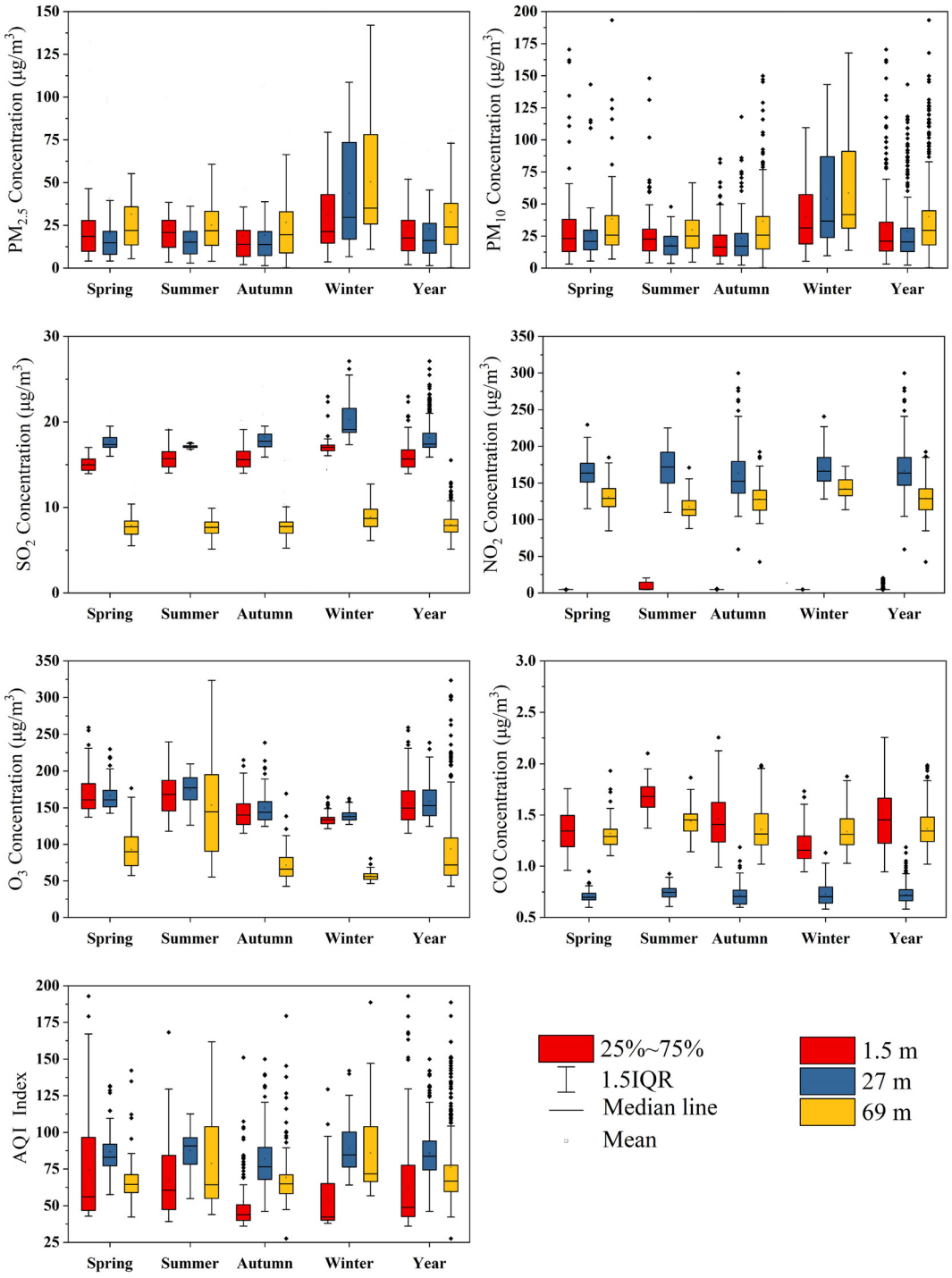

Fig. 2 – Air pollutant concentrations and the AQI in each season and for the entire year at three height levels in the urban street canyon (black dots represent outliers).

sumes a nonlinear relationship between an air pollutant concentration and environmental axes (Graffelman, 2001). It is used when the ordination of an air pollutant concentration matrix is constrained by a multiple regression on its relationships to environmental variables. The statistical significance of the CCA tests was obtained using a Monte Carlo simulation with 999 runs.

2. Results

2.1. *Air quality at the three height levels*

The concentrations of $PM_{2.5}$, PM_{10}, and SO_2 were each highest in winter (Fig. 2). Specifically, the highest wintertime $PM_{2.5}$

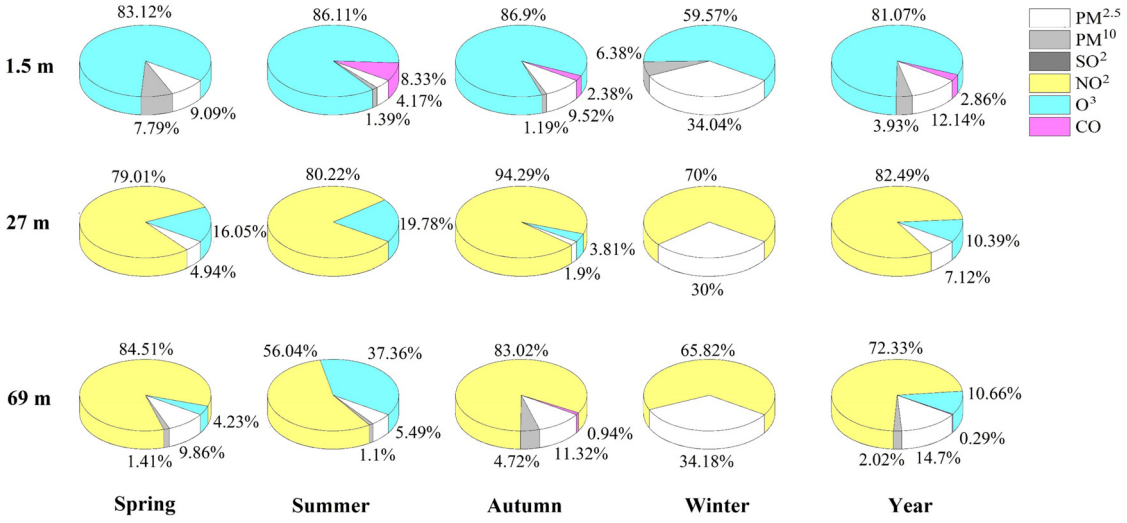

Fig. 3 – Percent of primary pollutants in each season and for the entire year at three height levels.

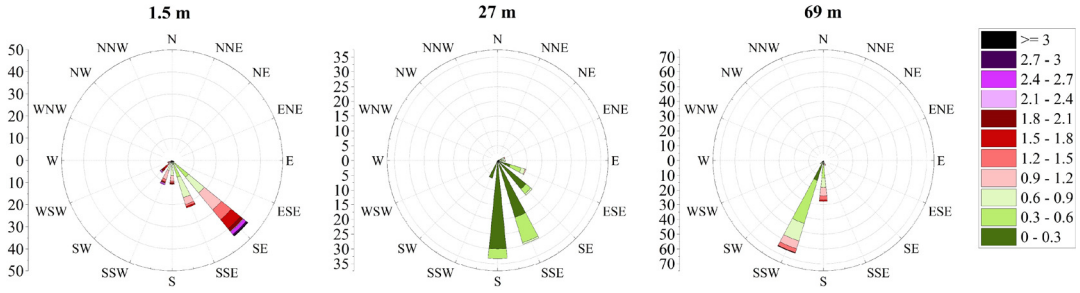

Fig. 4 – Wind rose plots including wind speed and direction at 1.5, 27 and 69 m.

concentration was 30.99 ± 3.27 μg/m^3 at 1.5 m, 43.93 ± 3.82 μg/m^3 at 27 m, and 50.30 ± 3.62 μg/m^3 at 69 m. The highest wintertime SO_2 concentration was 17.18 ± 0.21 μg/m^3 at 1.5 m, 20.24 ± 0.28 μg/m^3 at 27 m, and 8.89 ± 0.16 μg/m^3 at 69 m. However, the highest NO_2 concentration was 9.36 ± 0.68 μg/m^3 and 171.76 ± 2.78 μg/m^3 at 1.5 and 27 m in summer, respectively, and 142.45 ± 1.51 μg/m^3 at 69 m in winter. Moreover, the highest O_3 and CO concentrations were in summer. Specifically, the highest O_3 concentration was 167.45 ± 2.95 μg/m^3 at 1.5 m, 174.44 ± 2.14 μg/m^3 at 27 m, and 153.34±7.4 μg/m^3 at 69 m. The highest CO concentration was 1.68 ± 0.01 μg/m^3 at 1.5 m, 0.74 ± 0.01 μg/m^3 at 27 m, and 1.43 ± 0.01 μg/m^3 at 69 m.

Subsequent comparison of air pollutant concentrations between the three height levels revealed that the $PM_{2.5}$ concentration at 69 m was the highest during the entire year with a value of 32.67 ± 1.52 μg/m^3 (Fig. 2). The $PM_{2.5}$ concentration at 27 m was significantly higher than that at 1.5 m in winter, whereas it was lower than at that 1.5 m in other seasons. The SO_2 concentration during the entire year was 15.83 ± 0.84 μg/m^3 at 1.5 m, 18.15 ± 0.09 μg/m^3 at 27 m, and 8.01 ± 0.07 μg/m^3 at 69 m. Thus, the SO_2 concentration at 27 m was significantly higher than that at both 1.5 and 69 m in all seasons. The NO_2 concentration at 27 m was significantly higher than that at 69 m in all seasons, but both were more than 10 times higher than that at 1.5 m. The average values of O_3 concentration at 1.5 and 27 m were similar, however, the range of O_3 concentration at 1.5 m was larger than at that 27 m. The O_3 concentration at 69 m was the lowest among the three height levels with an average value of 93.82 ± 2.93 μg/m^3. The CO concentration at 27 m was half that at both 1.5 and 69 m in all seasons.

The yearly AQI at 27 m was 85.84 ± 0.93, i.e., significantly higher than that at 69 m, higher than that at 1.5 m (Fig. 2). There was no significant difference between the AQI at 27 m in spring, summer, and winter. The AQI in autumn was significantly lower than that in other seasons at all three height levels. The highest AQI at 1.5 and 69 m was 74.41 ± 4.11 in spring and 85.89 ± 3.23 in winter, respectively.

The percent of primary pollutants was calculated on the basis of the AQI component of each pollutant (Fig. 3). Days when O_3 was the primary pollutant at 1.5m accounted for 81.07% of the entire year. Days when NO_2 was the primary pollutant at 27 m and 69 m accounted for 82.49% and 72.33% of the entire year, respectively. The percent of days on which $PM_{2.5}$ was the primary pollutant at three height levels increased from summer to winter, and then decreased from winter to spring. However, the percent of days on which O_3 was the primary pollutant at the three height levels increased from spring to summer, and then decreased from summer to

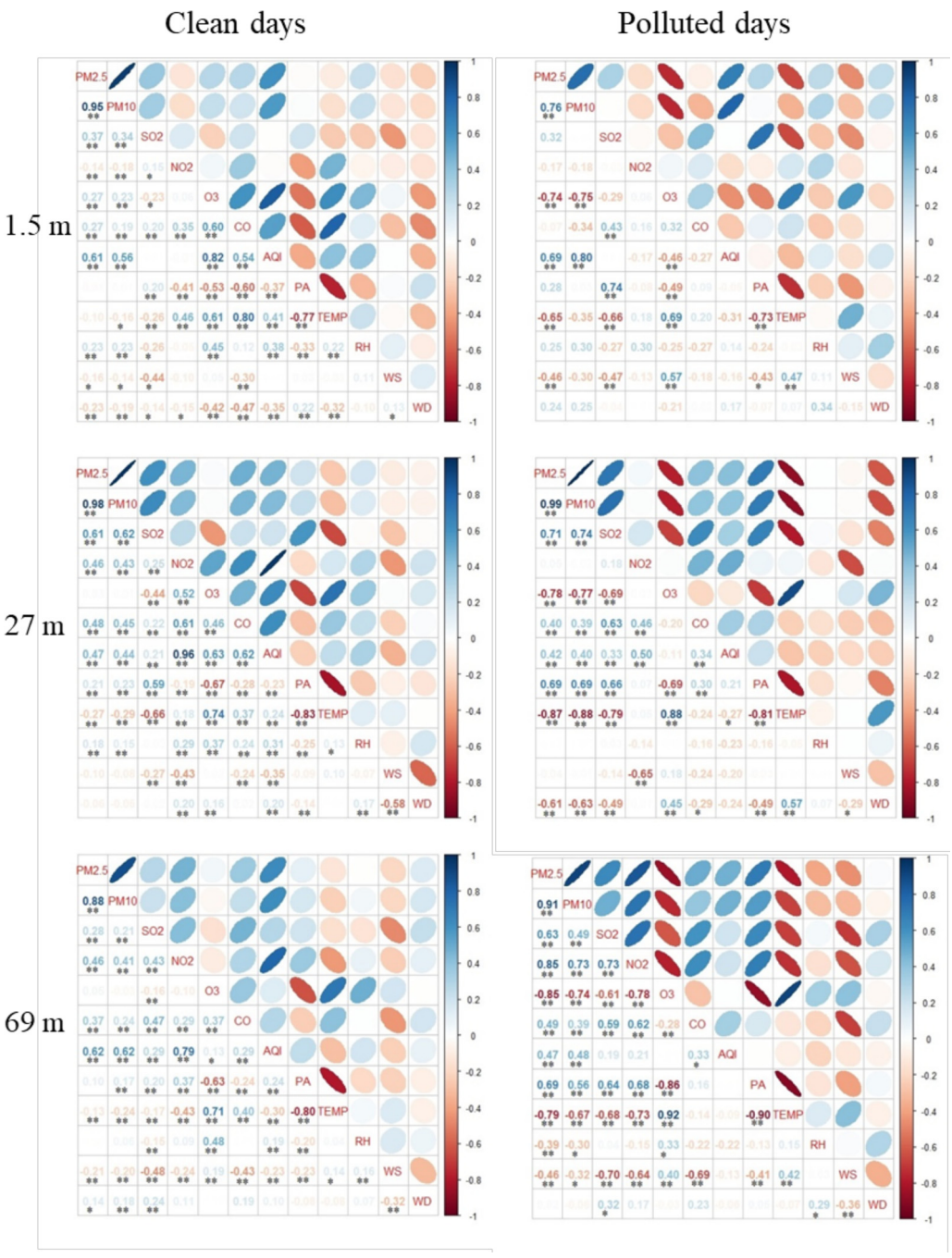

Fig. 5 – Pearson's correlations calculated between pairs of data of $PM_{2.5}$, PM_{10}, SO_2, NO_2, CO, AQI, atmospheric pressure (PA), air temperature (TEMP), relative humidity (RH), wind speed (WS) and wind direction (WD) at the three height levels on clean days and on polluted days. $p < 0.01$, * $p < 0.05$.**

winter. The highest percent of days on which CO was the primary pollutant (8.33%) at 1.5 m was in summer.

2.2. *Influence of microclimatic factors on air quality*

The wind speed and direction at 1.5, 27, and 69 m are shown in wind rose plots derived from daily data for the year (Fig. 4). The prevailing wind direction at 1.5, 27, and 69 m was SE, S, and SSW, respectively. The frequency of occurrence of the prevailing wind at 69 m was greater than that at both 1.5 and 27 m. The highest wind speed at 1.5 m was 3.02 m/sec, which was higher than that at both 69 (1.91 m/sec), and 27 m (1.44 m/sec). Moreover, the wind direction at 69 m was concentrated more in the direction of the prevailing wind than at both 1.5 and 27m.

The pairwise Pearson's correlation coefficients (r) between air pollutant concentrations and microclimatic factors on clean days and polluted days are shown in Fig. 5. Higher correlations were found between air temperature and $PM_{2.5}$, SO_2, and O_3 concentration on polluted days than on clean days. In

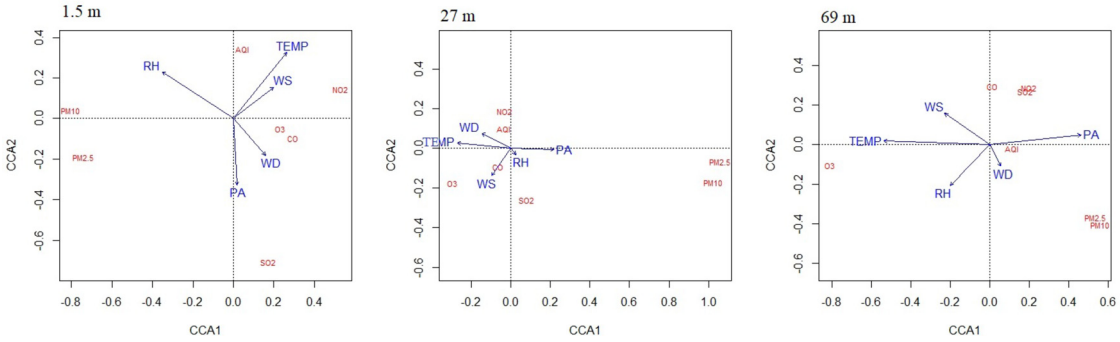

Fig. 6 – CCA biplot of $PM_{2.5}$, PM_{10}, CO, NO_2, SO_2, and O_3 concentrations and the AQI, and atmospheric pressure (PA), air temperature (TEMP), relative humidity (RH), wind speed (WS), and wind direction (WD) at 1.5, 27, and 69 m.

particular, higher negative correlations were found between air temperature and $PM_{2.5}$ at 1.5 m ($r = -0.65$), 27 m ($r = -0.87$) and 69 m ($r = -0.79$) on polluted days than at 1.5 m ($r = -0.10$), 27 m ($r = -0.27$) and 69 m ($r = -0.13$) on clean days. Also higher negative correlations were found between air temperature and SO_2 at 1.5 m ($r = -0.66$), 27 m ($r = -0.79$) and 69 m ($r = -0.68$) on polluted days than at 1.5 m ($r = -0.26$), 27 m ($r = -0.66$) and 69 m ($r = -0.17$) on clean days. However, higher positive correlations were found between air temperature and O_3 at 1.5 m ($r = 0.69$), 27 m ($r = 0.88$) and 69 m ($r = 0.92$) on polluted days than at 1.5 m ($r = 0.61$), 27 m ($r = 0.74$) and 69 m ($r = 0.71$) on clean days, whereas lower correlations were found between air temperature and CO at 1.5 m ($r = 0.20$), 27 m ($r = -0.24$) and 69 m ($r = -0.14$) on polluted days than at 1.5 m ($r = 0.80$), 27 m ($r = 0.37$) and 69 m ($r = 0.40$) on clean days.

The other microclimatic factors also showed different correlations with the air pollutants between clean and polluted days. For atmospheric pressure, positive correlation with SO_2 was found at 1.5 m ($r = 0.20$), 27 m ($r = 0.59$) and 69 m ($r = 0.20$) on clean days. Compared with clean days, higher positive correlations were found with all pollutants at 1.5 m ($r = 0.74$), 27 m ($r = 0.69$) and 69 m ($r = 0.64$) on polluted days. However, lower correlations was found between relative humidity and air pollutant concentrations on polluted days than on clean days at all three height levels. For wind speed, higher negative correlations with SO_2 were found at 1.5 m ($r = -0.47$) and 69 m ($r = -0.70$) on polluted days than at 1.5 m ($r = -0.44$) and 69 m ($r = -0.48$) on clean days. Also, higher negative correlations were found between wind speed and NO_2 at 27 m ($r = -0.65$) and 69 m ($r = -0.64$) on polluted days than at 27 m ($r = -0.43$) and 69 m (r = −0.24) on clean days. Moreover, microclimatic factors had lower correlations with the AQI on polluted days than on clean days at all three height levels.

The CCA plots show the main microclimatic factors that produced air pollutant and AQI variations at 1.5, 27, and 69 m (Fig. 6). CCA1 and CCA2 were the main components, explaining 96.3%, 98.7%, and 99.6% of the variance in air pollutant variability at 1.5, 27, and 69 m, respectively. Monte Carlo permutation tests on the correlation between the eigenvalues and air pollutant-microclimatic factors at 1.5 m for both components were significant ($p < 0.001$). For data at 1.5 m, CCA1 was positively associated with both wind speed and air temperature (weighted correlation coefficients between ordination component and environmental variables were 0.52 and 0.45, respectively), but negatively associated with both relative humidity and atmospheric pressure (−0.34 and −0.26, respectively). CCA2 was significantly associated with wind direction, atmospheric pressure, relative humidity, air temperature and wind speed (−0.99, −0.97, 0.94, 0.89 and 0.85, respectively). For data at 27 m, CCA1 was strongly conditioned by air temperature, atmospheric pressure, wind direction and wind speed (−0.98, 0.96, −0.82, and −0.65, respectively), while CCA2 was strongly correlated with relative humidity, wind speed and wind direction (−0.99, −0.75, and 0.56, respectively). For data at 69 m, CCA1 was significantly associated with wind speed, air temperature, atmospheric pressure, relative humidity, and wind direction (−0.99, 0.99, 0.98, −0.95, and 0.78, respectively), while CCA2 was correlated only with wind direction (−0.62) at 69 m.

The microclimatic factors including wind speed, wind direction, air temperature, relative humidity, and atmospheric pressure had significant influence on air pollutant variability at 1.5 m. Wind speed, wind direction, air temperature, and atmospheric pressure, rather than relative humidity, had significant influence on air pollutant variability at 27 m. Wind speed, air temperature, relative humidity, and atmospheric pressure, rather than wind direction, had significant influence on air pollutant variability at 69 m. The correlation coefficients calculated for 69 m were higher than those calculated for either 1.5 or 27 m, indicating that air pollutant concentrations depended on microclimatic factors more at 69 m than at either 1.5 or 27 m. Moreover, microclimatic factors explained the variability of chemical pollutants more than that of PM at all three height levels.

3. Discussion

3.1. *Vertical distribution of air pollutants*

Our study found that the concentration of PM at 1.5 m was higher than that at 27 m in spring, summer, and autumn, but lower in winter (Fig. 2). The higher concentration at 27 m in winter is consistent with the results of a previous study that found higher $PM_{2.5}$ and PM_{10} concentrations at 16 m than at 3 m in winter (Ezhilkumar and Karthikeyan, 2020). The difference between winter and other seasons might be attributable

to the variety of background concentrations and microclimatic factors. Low relative humidity and solar heating in winter greatly restrict upward transport of PM in street canyons (Lu et al., 2020). In this study, $PM_{2.5}$ and PM_{10} concentrations at roof level were significantly higher in winter than in other seasons (Fig. 2). Moreover, concentrations of $PM_{2.5}$ and PM_{10} in the street canyon were both higher than at roof level, indicating that particles diffused out of street canyon rather than accumulated within it. Low air temperature in winter reduced the mixing height, which resulted in inversion conditions and stable atmospheric conditions that trapped PM within the street canyon (Ganguly et al., 2019).

The distribution of chemical pollutants was different from that of PM in the street canyon (Fig. 2). The in-canyon PM concentration was lower than that at roof level, whereas the concentrations of SO_2, NO_2, and O_3 in the street canyon were higher than at roof level. Our results showed that chemical pollutants tended to accumulate in the street canyon. The ENVI-met model results showed larger difference between the output and the input concentrations for CO, NO_2, and O_3 than for PM (Li et al., 2021). The higher concentration of CO, NO_2, and O_3 were probably due to the contribution of motor vehicle emissions (Ezhilkumar and Karthikeyan, 2020). The hourly traffic volume is known to be an important indicator of NO_2 concentration in street canyons (Voordeckers et al., 2021b).

Overall, the concentrations of SO_2, NO_2, and O_3 increased and then decreased with height. Amato et al. (2019) reported shallow vertical deposition for NO_2. In contrast, the concentration of CO decreased and then increased with height, which might reflect the influence of vehicle emissions and human activities (Chen et al., 2018). Lu et al. (2020) also found a similar trend of CO concentration in urban residential areas of Shanghai. However, Zheng et al. (2021) reported an increase of CO concentration over a height range of 0–60 m on an open road. The difference can be explained by the complex ventilation effect of street canyons (He et al., 2019). A stable vortex can appear in a street canyon when the AR is > 0.7, a secondary flow can develop when AR reaches 2, and an inferior tertiary vortex can occur when AR is 3 (He et al., 2019). The AR of the studied site was approximately 2.3. In a real urban environment, high buildings can capture wind passing across an urban area and then wash it downward on both windward and leeward sides. Moreover, the different trends between photochemical pollutants (NO_2, and O_3) and CO probably reflect their complex photochemical reactions. At high temperature, photochemical reactions are active in areas close to building walls regardless of the flow pattern (Kwak and Baik, 2014).

According to Fig. 3, the primary pollutants in the studied urban street canyon in Shenyang were photochemical pollutants (i.e., NO_2 at 27 m and O_3 at 1.5 m). High exposure to NO_2 and O_3 pollution, rather than PM pollution, in the street canyon probably resulted from the high thermal conditions suitable for photochemical reactions attributable to diurnal wall heating scenarios in the canyon (Liu et al., 2021). The higher exposure to PM pollution in winter in comparison with other seasons was the result of coal burning for heating (Li et al., 2020). On those days on which CO was the primary pollutant, the highest concentration appeared at 1.5 m rather than at the other heights because of near-ground vehicle exhaust emissions. Overall, the difference in the AQI among the three height levels was similar to that of the photochemical pollutants, with the highest mean value at 27 m. Residents at 27 m suffered photochemical pollution in summer, and combined photochemical and PM pollution in winter. The highest AQI at 27 m was probably due to accumulation of air pollutants in the street canyon or exhaust fumes from the kitchens of residents (Ezhilkumar and Karthikeyan, 2020).

3.2. *Influence of microclimatic factors on air quality*

In comparison with clean days, the correlations between PM, SO_2, and the microclimatic factors increased on polluted days (Fig. 5). The vertical distribution of both PM and SO_2 was related to dispersion and deposition on clean days, whereas dependent on microclimatic factors on polluted days. Moreover, the microclimatic factors played important roles regarding PM and SO_2 concentrations at 1.5 and 69 m. Ezhilkumar and Karthikeyan (2020) also found strong correlation between the vertical trend of PM and microclimatic factors. Stronger negative correlations was found between PM and air temperature at the three height levels on polluted days than on clean days (Fig. 5). Low air temperature makes PM plumes stable within high-rise residential street canyons (Ezhilkumar and Karthikeyan, 2020).

In contrast to both PM and SO_2, the correlations between NO_2, O_3, and CO concentrations and the microclimatic factors were weakened on the polluted days, while the correlations between their concentrations at roof level and the microclimatic factors were enhanced (Fig. 5). Specifically, air temperature, wind speed, and wind direction, rather than relative humidity, influenced NO_2 and O_3 concentrations in the street canyon. Wind speed and wind direction played similar roles regarding the concentrations of NO_2 and O_3 in the street canyon, although wind speed rather than wind direction was the primary influence on the NO_2 and O_3 concentrations at 69 m. This means, irrespective of wind direction, the concentrations of NO_2 and O_3 at roof level were correlated with wind speed. However, the effects of both wind direction and wind speed were significant in determining the dispersion coefficients in the street canyon (Ganguly et al., 2019). Moreover, atmospheric pressure had greater effect on NO_2 concentration at roof level than on pollutant concentrations in the street canyon. The air pollutant concentrations at roof level were largely regulated by the dynamics of the local atmospheric boundary layer (Tiwari et al., 2013). The dispersion and distribution patterns of the photochemical pollutants in the street canyon were related to those factors that influence photochemical reactions and dispersion processes (Wu et al., 2019).

3.3. *Strengths and limitations*

The vertical distribution of air pollution in urban street canyons is strongly associated with high-rise cities that have experienced rapid urbanization (Eeftens et al., 2019). The current study obtained 1-year's observations of the vertical distribution of $PM_{2.5}$, PM_{10}, CO, NO_2, SO_2, and O_3 concentrations and microclimatic factors at three height levels in a N–S-oriented urban street canyon in Shenyang, China. The results could

provide reference information for studies considering the impact of the vertical characteristics of the built environment, and support the development of countermeasures intended to reduce the risk of exposure to heavy pollution for residents of street canyons.

The observation campaign was limited to three height levels in the street canyon because of the challenge to of encouraging a greater number of apartments to participate in the study. Although the limited number of observations allowed us to improve our understanding of the vertical distribution of pollution, the heights at which the concentrations of pollutants are highest or lowest remain unknown. Further 3D model simulation should be conducted to compensate the limited number of vertical observations, together with incorporation of local meteorological factors. Additionally, measured NO_2 concentrations at 27 and 69 m were much higher than at 1.5 m. Vertical observations using unmanned aerial vehicles in this street canyon should be conducted to verify these results. Moreover, air quality in an urban street canyon depends notably on traffic emissions (Minarro et al., 2012). The volume and speed of traffic should be considered to assess the vertical distribution of air pollutants in multiple street canyons with different AR and orientations.

4. Conclusions

In this study, a 1-year observational campaign was conducted to assess vertical air quality and its response to microclimatic factors in an urban street canyon in Shenyang, China. Results showed reduction in the concentration of PM with height in spring, summer, and autumn, whereas the PM concentration increased with height in winter. On clean days, PM tended to settle to the ground in the street canyon. However, the buildings along both sides of the canyon prevented PM from reaching the bottom of the canyon on polluted days. The in-canyon concentration of CO decreased with height, whereas the in-canyon concentrations of SO_2, NO_2, and O_3 increased with height in all seasons. Throughout the year, photochemical pollutants (NO_2 or O_3) represented the primary pollutants on more than 70% of. Their concentration at roof level was strongly correlated with atmospheric pressure, whereas the in-canyon concentration was determined by photochemical reactions and dispersion processes that were influenced by street canyon morphology.

Acknowledgments

This work was supported by the National Natural Science Foundation of China (Nos. 41730647, 41801187, 32101325), Youth Innovation Promotion Association CAS (No. 2022195). The authors wish to thank the anonymous reviewers for their valuable comments that helped to improve the manuscript.

Appendix A Supplemenary data

Supplementary data associated with this article can be found in the online version at doi:10.1016/j.jes.2022.02.021.

REFERENCES

Abhijith, K.V., Kumar, P., Gallagher, J., McNabola, A., Baldauf, R., Pilla, F., et al., 2017. Air pollution abatement performances of green infrastructure in open road and built-up street canyon environments - A review. Atmos. Environ. 162, 71–86.

Amato, F., Perez, N., Lopez, M., Ripoll, A., Alastuey, A., Pandolfi, M., et al., 2019. Vertical and horizontal fall-off of black carbon and NO_2 within urban blocks. Sci. Total Environ. 686, 236–245.

Chen, Y.C., Chang, C.C., Chen, W.N., Tsai, Y.J., Chang, S.Y., 2018. Determination of the vertical profile of aerosol chemical species in the microscale urban environment. Environ. Pollut. 243, 1360–1367.

Deshmukh, P., Kimbrough, S., Krabbe, S., Logan, R., Isakov, V., Baldauf, R., 2020. Identifying air pollution source impacts in urban communities using mobile monitoring. Sci. Total Environ. 715, 136979.

Ding, Z.N., Chen, H.Y., Zhou, L.G., 2021. Optimal group selection algorithm in air quality index forecasting via cooperative information criterion. J. Clean. Prod. 283, 125248.

Eeftens, M., Odabasi, D., Fluckiger, B., Davey, M., Ineichen, A., Feigenwinter, C., et al., 2019. Modelling the vertical gradient of nitrogen dioxide in an urban area. Sci. Total Environ. 650, 452–458.

Eslami, T., Saeed, F., 2018. Fast-GPU-PCC: a gpu-based technique to compute pairwise Pearson's correlation coefficients for time series data—fMRI study. High-Throughput 7, 11.

Ezhilkumar, M.R., Karthikeyan, S., 2020. Vertical measurement of $PM_{2.5}$ and PM_{10} in street canyons and cohort health risk estimation at Chennai, South India. Environ. Eng. Sci. 37 (8), 535–547.

Fu, X.W., Xiang, S.L., Liu, Y., Liu, J.F., Yu, J., Mauzerall, D.L., et al., 2020. High-resolution simulation of local traffic-related NOx dispersion and distribution in a complex urban terrain. Environ. Pollut. 263, 114390.

Ganguly, R., Sharma, D., Kumar, P., 2019. Trend analysis of observational PM_{10} concentrations in Shimla city. India. Sustain. Cities Soc. 51, 101719.

Graffelman, J., 2001. Quality statistics in canonical correspondence analysis. Environmetrics 12 (5), 485–497.

Hassan, A.M., ELMokadem, A.A., Megahed, N.A., Eleinen, O.M.A., 2020. Urban morphology as a passive strategy in promoting outdoor air quality. J. Biuld Eng. 29, 101204.

He, B.J., Ding, L., Prasad, D., 2019. Enhancing urban ventilation performance through the development of precinct ventilation zones: A case study based on the Greater Sydney, Australia. Sustain. Cities Soc. 47, 101472.

He, H.D., Gao, H.O., 2021. Particulate matter exposure at a densely populated urban traffic intersection and crosswalk. Environ. Pollut. 268, 115931.

Huang, Y.D., Hou, R.W., Liu, Z.Y., Song, Y., Cui, P.Y., Kim, C.N., 2019. Effects of wind direction on the airflow and pollutant dispersion inside a long street canyon. Aerosol. Air Qual. Res. 19 (5), 1152–1171.

Kwak, K.H., Baik, J.J., 2014. Diurnal variation of NOx and ozone exchange between a street canyon and the overlying air. Atmos. Environ. 86, 120–128.

Li, C., Liu, M., Hu, Y., Zhou, R., Huang, N., Wu, W., et al., 2020. Spatial distribution characteristics of gaseous pollutants and particulate matter inside a city in the heating season of Northeast China. Sustain. Cities Soc. 61, 102302.

Li, P.P., Miao, C.P., Chen, W., Hu, Y.M., He, X.Y., 2021. Numerical simulation on the influence of street tree on $PM_{2.5}$ concentration in the street canyon. Chin. J. Ecol doi:10.13292/j.1000-4890.202111.036.

Li, Z.Y., Fung, J.C.H., Lau, A.K.H., 2018. High spatiotemporal characterization of on-road $PM_{2.5}$ concentrations in

high-density urban areas using mobile monitoring. Build. Environ. 143, 196–205.
Liaoning Shenyang ecological environment monitoring center, Shenyang Environmental Quality Bulletin in the first half of 2020. http://sthjj.shenyang.gov.cn/html/STHJJ/15686251845 3996/156862518453976/160879431280661/1845399609165462. html.
Liu, J., Cui, S., Chen, G., Zhong, Y., Wang, X., Wang, Q., et al., 2021. The influence of solar natural heating and NOx-O_3 photochemistry on flow and reactive pollutant exposure in 2D street canyons. Sci. Total Environ. 759, 143527.
Lu, K.F., He, H.D., Wang, H.W., Li, X.B., Peng, Z.R., 2020. Characterizing temporal and vertical distribution patterns of traffic-emitted pollutants near an elevated expressway in urban residential areas. Build. Environ. 172, 106678.
Miao, C., Yu, S., Hu, Y., Bu, R., Qi, L., He, X., Chen, W., 2020a. How the morphology of urban street canyons affects suspended particulate matter concentration at the pedestrian level: an in-situ investigation. Sustain. Cities Soc. 55, 102042.
Miao, C., Yu, S., Hu, Y., Liu, M., Yao, J., Zhang, Y., et al., 2021. Seasonal effects of street trees on particulate matter concentration in an urban street canyon. Sustain. Cities Soc. 73, 103095.
Miao, C., Yu, S., Hu, Y., Zhang, H., He, X., Chen, W., 2020b. Review of methods used to estimate the sky view factor in urban street canyons. Build. Environ. 168, 106497.
Minarro, M.D., Terres, I.M.M., Egea, J.A., Ferradas, E.G., Aznar, A.M., 2012. Vertical concentration gradients of volatile organic compounds in two NS-oriented street canyons. Environ. Monit. Assess. 184 (12), 7353–7364.
Ming, T.Z., Shi, T.H., Han, H.N., Liu, S.R., Wu, Y.J., Li, W.Y., et al., 2021. Assessment of pollutant dispersion in urban street canyons based on field synergy theory. Atmos. Pollut. Res. 12 (2), 341–356.
Moradpour, M., Afshin, H., Farhanieh, B., 2018. A numerical study of reactive pollutant dispersion in street canyons with green roofs. Build Simul-China 11 (1), 125–138.
Oke, T.R., 1988. Street Design and Urban Canopy Layer Climate. Energ Build. 11 (1-3), 103–113.
Shi, Y., Xie, X.L., Fung, J.C.H., Ng, E., 2018. Identifying critical building morphological design factors of street-level air pollution dispersion in high-density built environment using mobile monitoring. Build. Environ. 128, 248–259.
Tan, X.R., Han, L.J., Zhang, X.Y., Zhou, W.Q., Li, W.F., Qian, Y.G., 2021. A review of current air quality indexes and improvements under the multi-contaminant air pollution exposure. J. Environ. Manage. 279, 111681.
Tao, Y., Zhang, Z., Ou, W.X., Guo, J., Pueppke, S.G., 2020. How does urban form influence PM2.5 concentrations: Insights from 350 different-sized cities in the rapidly urbanizing Yangtze River Delta region of China, 1998-2015. Cities 98, 102581.
Terbraak, C.J.F., 1986. Canonical correspondence-analysis - a new eigenvector technique for multivariate direct gradient analysis. Ecology 67 (5), 1167–1179.
Tiwari, S., Srivastava, A.K., Bisht, D.S., Parmita, P., Srivastava, M.K., Attri, S.D., 2013. Diurnal and seasonal variations of black carbon and $PM_{2.5}$ over New Delhi, India: Influence of meteorology. Atmos. Res. 125, 50–62.
Tomson, M., Kumar, P., Barwise, Y., Perez, P., Forehead, H., French, K., et al., 2021. Green infrastructure for air quality improvement in street canyons. Environ. Int. 146, 106288.
Voordeckers, D., Lauriks, T., Denys, S., Billen, P., Tytgat, T., Van Acker, M., 2021a. Guidelines for passive control of traffic-related air pollution in street canyons: An overview for urban planning. Landsc. Urban Plan. 207, 103980.
Voordeckers, D., Meysman, F.J.R., Billen, P., Tytgat, T., Van Acker, M., 2021b. The impact of street canyon morphology and traffic volume on NO_2 values in the street canyons of Antwerp. Build. Environ. 197, 107825.
Wen, H., Malki-Epshtein, L., 2018. A parametric study of the effect of roof height and morphology on air pollution dispersion in street canyons. J. Wind Eng. Ind. Aerod. 175, 328–341.
Wu, W., Li, L.D., Li, C.L., 2021. Seasonal variation in the effects of urban environmental factors on land surface temperature in a winter city. J. Clean. Prod. 299, 126897.
Wu, Y.H., Zhao, K.H., Huang, J.P., Arend, M., Gross, B., Moshary, F., 2019. Observation of heat wave effects on the urban air quality and PBL in New York City area. Atmos. Environ. 218, 117024.
Yang, J.Y., Shi, B.X., Shi, Y., Marvin, S., Zheng, Y., Xia, G.Y., 2020. Air pollution dispersal in high density urban areas: Research on the triadic relation of wind, air pollution, and urban form. Sustain. Cities Soc. 54, 101941.
Zheng, T., Li, B., Li, X.B., Wang, Z.Y., Li, S.Y., Peng, Z.R., 2021. Vertical and horizontal distributions of traffic-related pollutants beside an urban arterial road based on unmanned aerial vehicle observations. Build. Environ. 187, 107401.